Aalborg Universitet

THE LARGE OFFICE ENVIRONMENT - MEASUREMENT AND MODELING OF THE WIDEBAND RADIO CHANNEL

J. Bach Andersen, J. Ø. Nielsen
Aalborg University
Niels Jernes Vej 12, 9220 Aalborg
Denmark
jba,jni@kom.aau.dk

G. Bauch, M. Herdin
DoCoMo Euro-Labs
Landsbergerstr. 312, Munich
Germany
bauch,herdin@docomolab-euro.com

ABSTRACT

In a future 4G or WLAN wideband application we can imagine multiple users in a large office environment consisting of a single room with partitions. Up to now, indoor radio channel measurement and modelling has mainly concentrated on scenarios with several office rooms and corridors. We present here measurements at 5.8GHz for 100 MHz bandwidth and a novel modelling approach for the wideband radio channel in a large office room environment. An acoustic like reverberation theory is proposed that allows to specify a tapped delay line model just from the room dimensions and an average absorption coefficient of the delimiting walls. The proposed model agrees amazingly well with the measurements, showing that the diffuse part is uniformly spread over the room with a constant energy level and a constant temporal decay slope. Furthermore, we analyze fading statistics and capacities calculated from the measurements. The proposed model can likely also be applied to indoor hot spot scenarios.

I. INTRODUCTION

Most early work on indoor propagation was related to narrowband pathloss studies describing the impact of floors and walls between rooms. An overview of the indoor radio channel up to 1992 is given in [2] with an extensive bibliography.

The Saleh-Valenzuela work [1] was one of the early ones making a wideband model based on measurements in a building. It was important in the sense of introducing the cluster concept, where a cluster is a collection of rays decaying exponentially in time. The clusters and the rays within were modeled by a Poisson distribution of arrival times. The measurements were made at 1.5 GHz with a 10 ns pulse, similar to the bandwidth in this study. The transmitter was placed in a long corridor and the receivers moved around in offices connected to the corridor. In most cases the clusters were formed by the building superstructure, such as reflections from metal doors at the end of the corridor. Excluding such cases a single cluster with high density of rays over the entire time axis appeared. In the present study, we consider a different indoor scenario, namely a large office room environment with room partitions where each receive position has close to line-of-sight to the transmitter. Such an environment would typically have many users in a wideband wireless (MIMO) system. As we shall see, this leads to a significantly different characterization of the radio channel. The cluster concept was extended to the angular domain in [3] based on measurements around 7 GHz and a resolution of 3 ns. In that case the transmitter and receiver were in different rooms like in most other studies.

There are only few papers on the single room channel. In [4] some bounds are derived for the mean received power, when both receiver and transmitter may be randomly positioned. Interestingly, the bounds involve the surface area and the volume, as known from room acoustics, although the authors do not refer to this.

While most indoor studies of the wideband channel for buildings as such, consisting of corridors, halls and offices, show that clusters can be identified; this is not the case for the large office room environment. As we shall show, clustering appears only for the very beginning of the impulse response. A major part of the impulse response can be described by exponential decay due to diffuse scattering [5]. A stochastic approach for indoor diffuse scattering is described in [10] treating pathloss distributions. Extracting diffuse scattering from measurements is discussed in [8], and recently ultra-wideband diffuse scattering has been measured in several rooms [9]. In the present paper we concentrate on modeling the wideband channel for the link between an access point placed in the ceiling of the room and users placed in a number of positions around the room. Although, we present also some analysis regarding the spatial structure of the channel, the major focus lies on the delay domain.

The paper is organized as follows. After a description of the environment and the measurements the narrowband properties are described in section III, and the wideband delay and angle properties in section IV and V. The exponential tail of the responses is treated theoretically in section VI, a simple tap delay line model in section VII, the ergodic capacities in section VIII, and a conclusion terminates the paper.

II. THE ENVIRONMENT

The room is a rectangular room with dimensions 11*20*2.5 meters with windows at two sides, wall A and C, and filled with cardboard partitions with metallic frames; an overview drawing is seen in Fig. 1. Other elements were book cases, tables, chairs and computers. The transmitter (AP1) was positioned near the ceiling at the middle of the room, and the 11 positions of the receivers are indicated on the drawing. A few measurements were also made with AP4 at the left side of the room.
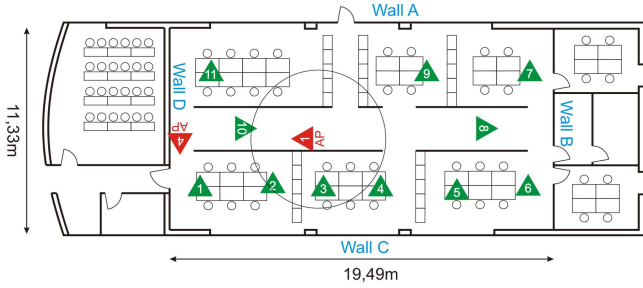

Figure 1. A single room office environment. 11 user locations and 2 access points (AP1 and AP4). The circle indicates the reverberation distance around AP1.

The antennas were monopole arrays with additional parasitic elements, the transmit array with 16 (4*4) active elements looking downwards from the ceiling and the receive array with 32 (4*8) elements looking upwards. The antennas have a maximum gain around 45 ° elevation angle and a loss of 1.5 dB due to coupling to loaded neighbor elements. The frequency was 5.8 GHz and the bandwidth of operation was 100 MHz. The whole receiver array could be moved on a sledge The channel sounder is further described in [7].

III. NARROWBAND RESULTS

A. Path gains

The overall path loss or path gain of the various sites is the most important link parameter. Here the mean power at a single frequency is obtained as an average over all antennas on both sides and receiver positions, and compared with the back-to-back measurement of the transmitted power. The results for AP1 are shown in Fig.2.

In general the path gains follow the free space law including the antenna gains, exactly for the nearest points at 3-5 meters distance, while the others have an excess loss of 0-8 dB due to local shadowing.

B. Power distributions

The local narrowband fading distributions are important indicators for the channel properties, whether they are Rayleigh, Rice or something else. The results for the 10 locations and AP1 are shown in Fig. 3 (there are 11 locations but the measurements from position 10 are not available). Cumulative distributions are shown on a log scale,

and the powers are normalized to a mean power of one, zero dB.
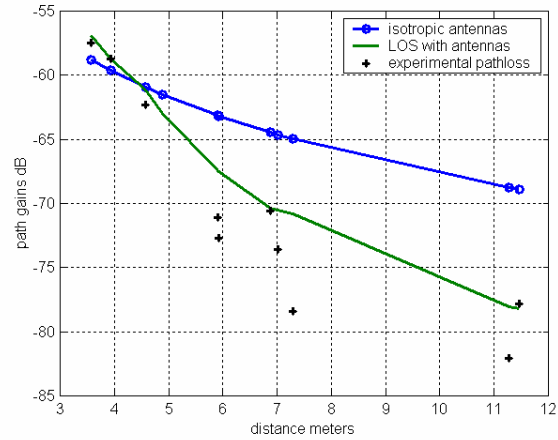

Figure 2. Path gains from access point 1 as a function of LOS distance. Upper curve (o) is free space path gain with isotropic antennas, lower curve including the antenna gains, and the crosses (+) the measured values.
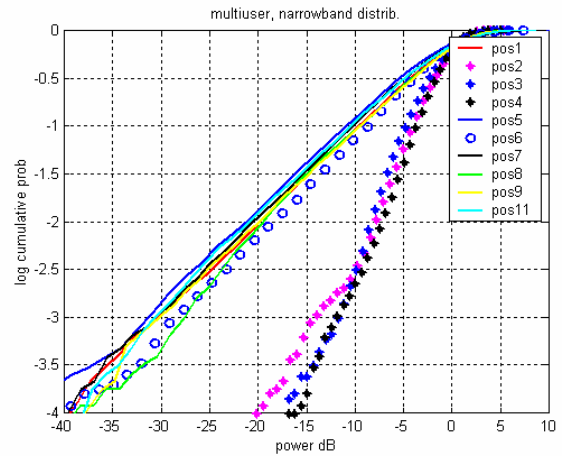
Figure 3 Cumulative distributions at ten locations from AP1. Curves with (+) have Ricean distributions and belong to positions 2, 3 and 4 close to the access point. The remaining are close to Rayleigh. The mean powers are normalized to 0 dB

It is clear that the distributions fall in two groups, one group with close to Rayleigh distribution and another group Ricean with a K-factor of around 9 dB. The locations belonging to the Ricean group are close to the access point (see Fig. 2), about 4 meters, which is important for the later discussions of the diffuse energy.

IV. WIDEBAND RESULTS

The mean power delay profiles as shown in Fig.4 are averages over all antenna positions and elements. The zero delay corresponds to the peak of the transmitter impulse, and it is seen that all locations are characterized by a rapid rise to a peak value and then followed by a decay. The decay is exactly exponential for most locations and close to exponential for the three outlier positions, 2, 3 and 4, shown as dashed lines. For those locations furthest away from the transmitter the rise naturally comes last, as for positions 6 and 7 in the right corners, so the absolute delay is included.
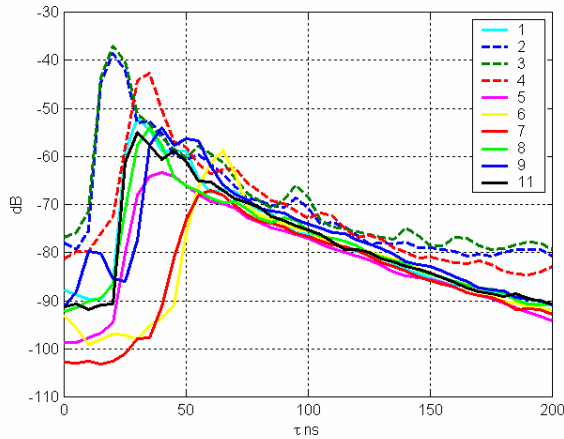

Figure 4. Mean power delay profiles for different receiver locations with AP1 as transmitter. Dashed profiles belong to the three Rice distribution locations (Fig. 1). Zero delay corresponds to peak impulse at the transmitter.

It should be noted that the apparent floor for the dashed curves is due to the limited dynamic range of the equipment, so it is a noise floor, not to be considered as a propagation phenomenon. Removing the three dashed curves makes a much clearer picture as seen in Fig. 5.
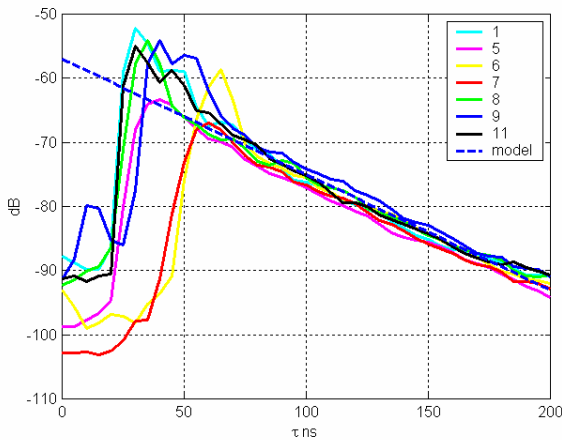

Figure 5 Same as Fig. 4 without the three 'Ricean' locations. Dashed line is the theoretical result for the diffuse field.

The impulse responses in Fig. 5 now share a common exponential tail, not only in slope (0.18 dB/ns), but also in magnitude. This is at first glance surprising but is in perfect agreement with the diffusion theory in section VI. If the tail is extrapolated backwards we find that the peaks have an offset above the tail from 1 to 10 dB.

V. ANGULAR ASPECTS

The angular aspects are important for the antenna correlations and MIMO capacity in general. Space does not permit a thorough exposition of the angular aspects, but an example will illustrate the phenomena. The delay-angle response is found by a simple angular beam scan at the receiver array (4*8 elements) for each 10 ns of the delay variable. This is done for all values of transmitter antenna elements and the mean value is found. A typical example is shown in Fig. 6. The main result is that there is a certain peaking of the radiation in the beginning of the impulse, but that after some delay the energy is uniformly distributed in angle. This again supports a diffusion theory where the energy in the tail is uniformly distributed in space and on average uniformly distributed in angle.
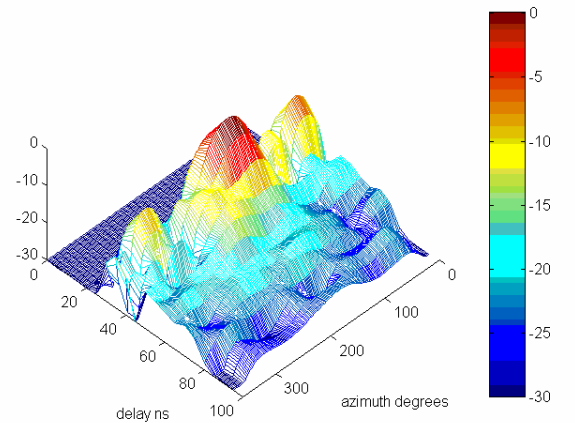
Figure 6. Delay-angle response at position 9.

VI. THEORY OF DIFFUSE POWER

A. Energy density and path gain

The experimental results as shown in Figs. 5 and 6 bear a great similarity to what is known about acoustic reverberations in a room. We have therefore translated the acoustical theory to electromagnetics, where the details may be found in [5] and only key results given here.
Assume from the onset that the energy is evenly distributed over the room and at a given point the incident angles are uniformly distributed. Then the result is the following for the time response of the energy density after the source is turned off,

$$W(\tau) = W_0 e^{-\tau/s}$$
$$s = \frac{4V}{c\eta A} \qquad (1)$$

The only difference from the acoustics case is the velocity of light c instead of the velocity of sound [6]. V is the volume of the room, A the total area including floor and ceiling, and η an average absorption coefficient of the walls. In practice it would also include absorption in furniture and persons. The delay time s, called the reverberation time, may be found from the experiments (Fig 5) to be 24.1 ns. From (1) we can determine η, the only unknown, to be 0.51.

It is also possible to determine the path gain of the diffuse power [5]

$$\frac{P_{diffuse}(\tau)}{S} = \frac{\lambda^2}{\pi\eta A} e^{-\tau/s} \qquad (2)$$

where S is the input power, $P_{diffuse}$, the power received by the receiving antenna, and λ the wavelength corresponding to the carrier frequency. Note that the received diffuse power is independent of the antennas, since the distributed directivity in such an environment is unity. Calculating the gain for the specific room and the given parameters we find a gain of -57 dB at $\tau=0$ after having subtracted the antenna efficiencies, in perfect agreement with the experimental results in Fig. 5, dashed curve.

It is also of interest to use another position of the access point in the same room. Fig. 7 shows the power delay profiles for some of the locations similar to Fig. 5, but for AP4 at the extreme left side of the room.
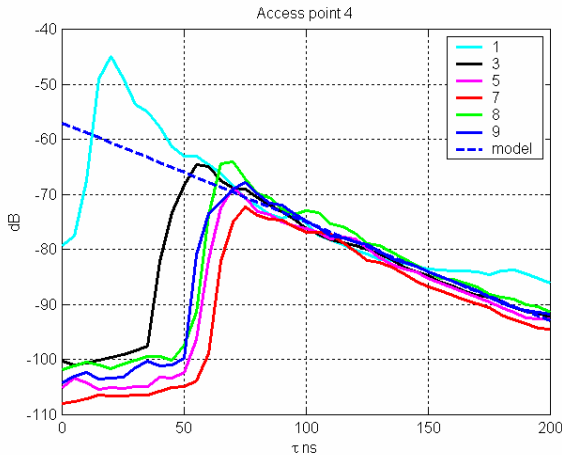

Figure 7. Similar to Fig. 5 but with the access point AP4 near an end wall

The results for the tails are exactly the same. It is a good evidence for the validity of the model that not only are the response tails independent of the position of the users, but also of the position of access point.

B. Reverberation distance

It is clear that very near the transmit antenna there will be a strong line-of-sight field dominating over the diffuse field. The power received from the transmit antenna will be

$$P_{dir} = \frac{SD_1 D_2}{4\pi r^2} \frac{\lambda^2}{4\pi} \qquad (3)$$

where D_1 and D_2 are the two directivities, the standard Friis formula.

Using (2) for $\tau=0$ and (3) we can find the distance where the two powers are equal. This distance is called the reverberation distance, and is given by

$$r_d = \frac{1}{4}\sqrt{\frac{D_1 D_2 \eta A}{\pi}} \qquad (4)$$

For distances closer than r_d the direct path dominates, for larger distances the diffused energy dominates. Due to the changing directivities r_d varies over the room from 2 to 4 meters. The reverberation distance for access point 1 is indicated as a circle in Fig. 1. The so-called Ricean positions with a Rice distribution with a significant K-factor are exactly those points within or near the circle. This explains then why all the remaining positions (Fig. 3) have near Rayleigh distributions; they are dominated by the diffuse field.

VII.   TAP DELAY LINE MODEL

Based on the results of the previous sections we can now formulate a channel model, which should have general validity for this type of room.

The first tap controls the peak of the pulse which arrives after a certain delay, which is correlated to the distance. The distribution of the tap magnitude is Ricean with a K-factor which may be zero (Rayleigh). The peak has a certain offset above the diffuse power. In a geometrical channel model the directional distribution for the first tap is chosen to peak in the direction of the access point with a certain angular spread.

All the other taps, on which we have concentrated in this paper, are characterized by a much simpler model. The taps decrease exponentially corresponding to the reverberation time of the room, the envelope distribution is Rayleigh, and the directional distribution is uniform over all angles. The model is sketched n Fig. 8. A more refined model could have more than one tap for the non-diffuse part.

VIII. CAPACITY

Although the emphasis in the paper is on the channel model, it is still of interest to see the impact of the diffusion on the capacity in the room.

Fig. 9 shows the ergodic capacities for the full 16*32 matrix in b/s/Hz as a function of assumed SNR values calculated on the basis of the experimental channel measurements.
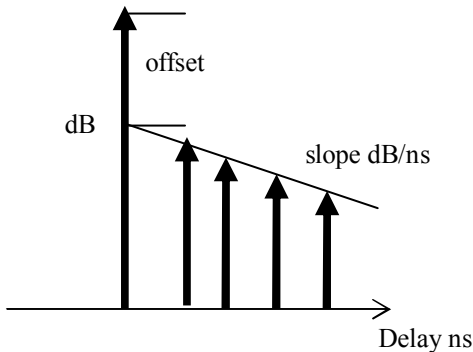

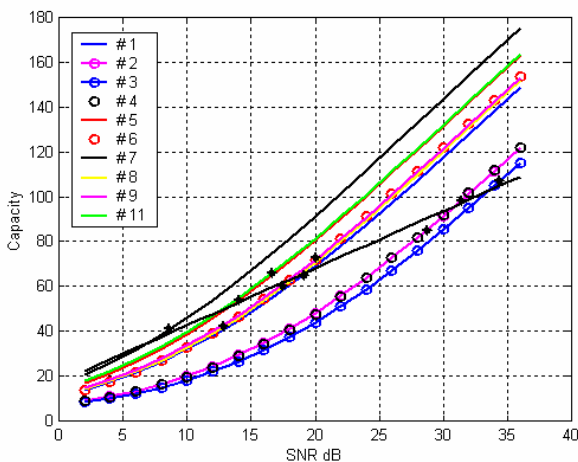*Figure 8 Tap delay line model*

Figure 9. Ergodic capacities in the room for various locations based on the measured channel matrices. Assuming one location has an SNR of 20 dB the remaining locations are allocated correct relative SNRs corresponding to the path gains and the corresponding capacities are shown as +. The line is best fit through the crosses.

It is clear that we again get a grouping of the Rice-locations with a high K-factor and consequent low richness and the Rayleigh group with higher richness (capacity for fixed SNR). For fixed SNR definitely the Rayleigh group is superior as expected. However, if instead we address the situation with a fixed transmit power the situation changes and SNR varies according to the path gains found earlier. In Fig. 9 we have assumed that one location in the middle has an SNR of 20 dB and allocated the other positions accordingly, and the capacity versus SNR is then close to a linear relationship. The locations with high diffuse content have high richness but low SNR, and contrary the locations with most power and little diffuse content has the highest capacity. Power is more important than richness. Further discussion on this may be found in [11].

IX. CONCLUSION

The channel characteristics of a large office room have been analyzed experimentally and theoretically. The emphasis has been on the delay characteristics, where it has been shown that an acoustic like model of reverberation explains in great detail the exponentially decaying tail of the impulse. The properties of the tail are independent of location, both in slope and magnitude. The concept of reverberation distance is important since the distance separates the regions of Ricean and Rayleigh distributed envelopes for the total energy, and in this particular case also regions with high capacity from those of lower capacity for fixed transmit power.

X. REFERENCES

[1] A. M. Saleh and R. A. Valenzuela, "A Statistical Model for Indoor Multipath Propagation", *IEEE Journal of Selected Areas in Communications,* vol. 5, no 2, February 1987, pp 128-137

[2] H. Hashemi, "The Indoor Radio Propagation Channel", *Proc. IEEE,* vol. 81, no 7, July 1993, pp 943-968

[3] Q. Spencer, B. Jeffs, M. Jensen, A.L. Swindlehurst, "Modelling the Statistical Time and Angle of Arrival Characteristics of an Indoor Multipath Channel", *IEEE Journal on Selected Areas in Communications*, Volume 18, Issue 3, March 2000, pp 347 - 360

[4] J. Hansen and P. Leuthold, "The Mean Received Power in *AdHoc* Networks and its Dependence on Geometrical Quantities", *IEEE Trans. on Antennas and Propagation,* vol 51., no 9, September 2003, pp 2413-2419

[5] J. Bach Andersen, J. Ø. Nielsen, G. Bauch and M. Herdin, „ Room Electromagnetics", submitted 2006

[6] H. Kuttruff, *Room Acoustics,* fourth edition, Spon Press, 2000

[7] J. Ø. Nielsen, J. B. Andersen, P. C. F. Eggers, G. F. Pedersen, K. Olesen, E. H. Sørensen, and H. Suda, "Measurements of indoor 16*32 wideband MIMO channels at 5.8 GHz", *Proceedings of the 2004 Symposium on Spread Spectrum Techniques and Applications (ISSSTA 2004),* pp 864-868

[8] A. Richter, R.S. Thomä, "Joint maximum likelihood estimation of specular paths and distributed diffuse scattering", *Proc. IEEE Vehicular Technology Conference,* vol 1, Stockholm, May, 2005, pp. 11-15

[9] J. Kunisch and J. Pamp, "Measurement results and modeling aspects for the UWB radio channel, *Proc. IEEE Conference on Ultra Wideband Systems and Technologies*, May 2002, pp. 19-23

[10] D. Ullmo and H.U. Baranger, "Wireless Propagation in Buildings: A Statistical Scattering Approach", *IEEE Trans. on Vehicular Technology,* vol. 48,, no 3,May 1999, pp 947-955

[11] J.Ø.Nielsen, J.B.Andersen, G. Bauch, M. Herdin, „Relationship between capacity and pathloss for indoor MIMO channels", this conference